



Figures and figure supplements

SUMOylation of $\text{Na}_v1.2$ channels mediates the early response to acute hypoxia in central neurons

Leigh D Plant et al

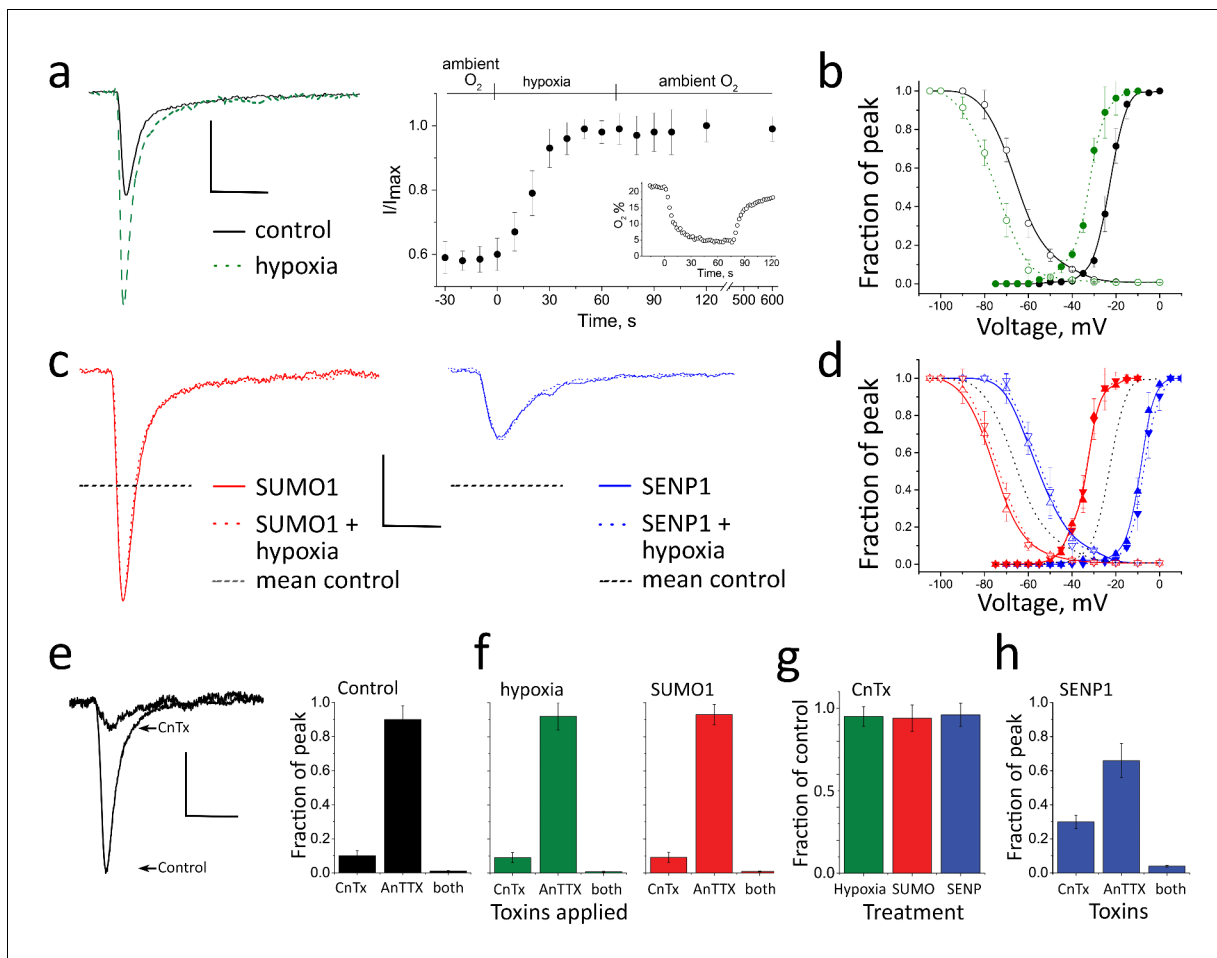


Figure 1. Acute hypoxia and SUMO1 augment I_{Na} in rat CGN. I_{Na} in rat CGN was studied by whole-cell patch-clamp. Normalized activation (Act) and steady-state inactivation (SSI) relationships were obtained and fit as described in the Materials and methods. Measured values are noted in the text and listed in **Table 1**. The time-course of hypoxic modulation of I_{Na} was studied by steps from -100 mV to -20 mV every 10 s. Cells were studied with control solution (black), 100 pM SUMO1 (red), or 250 pM SENP1 (blue) in the recording pipette. To assess the relative contributions of $Na_v1.2$ and $Na_v1.6$ channel currents to I_{Na} , 250 nM μ -conotoxin TIIIA (CnTx) and 50 nM 4,9 anhydro-TTX (anTTX) were applied as indicated. Data are mean \pm S.E.M. for 10 to 15 cells per group. Scale bars are 150 pA/pF and 5 ms for panels a to d, and 75 pA/pF and 5 ms in panel e. (a) Left, example traces showing I_{Na} at -20 mV increased when control perfusate at 21% O_2 (black) was exchanged with a hypoxic solution at 5% O_2 (---). Right, the time-course for changes in the peak current in response to decreased O_2 , and on return to normoxia (washout), is shown normalized to the maximal current for each cell studied. Inset, The level of O_2 was measured in real-time in the recording chamber and fell from 21 to 5% within 18 ± 1 s (o). Error bars are within the symbols. (b) Hypoxic solution (green dashes) left shifted the $V_{1/2}$ of I_{Na} from control (black) for both Act (solid) and SSI (open). (c) Left, SUMO1 in the pipette (red) increased I_{Na} and no further augmentation was observed by subsequent hypoxia (red dashes). Right, SENP1 in the pipette (blue) decreased I_{Na} and suppressed the response to hypoxia (blue dashes). Dotted black lines indicate the mean peak values in control normoxic solutions from a. (d) SUMO1 left shifted the $V_{1/2}$ of Act (red triangle) and SSI (open red triangle). The relationships were then insensitive to hypoxia (Act, red down triangle; SSI, open red down triangle). SENP1 right shifted the $V_{1/2}$ of Act (blue triangle) and SSI (open blue triangle) and currents were then insensitive to hypoxia. Dashed black lines indicate mean peak values with control solutions from b. (e) Left, I_{Na} traces under control conditions and with toxins in the bath. Right; mean normalized peak current histograms showing $90 \pm 0.8\%$ inhibition by CnTx, $10 \pm 0.3\%$ inhibition by AnTTX and $98 \pm 0.02\%$ inhibition by both toxins with 21% O_2 (black bars). (f) Mean normalized peak I_{Na} histograms. Left; $92 \pm 1\%$ inhibition by CnTx and $9 \pm 1\%$ inhibition by AnTTX with a drop to 5% O_2 for 60 s (green). Right; $93 \pm 2\%$ inhibition by CnTx and $7 \pm 1\%$ inhibition by AnTTX with 100 pM SUMO1 in the pipette (red). (g) Mean normalized peak current histograms show that the I_{Na} remaining after inhibition of $Na_v1.2$ by CnTx did not respond to acute hypoxia at 5% O_2 (green), SUMO1 (red) or SENP1 (blue). (h) Mean normalized peak I_{Na} histograms with SENP1 in the pipette with 21% O_2 (blue) showing $70 \pm 4\%$ inhibition by CnTx, $34 \pm 8\%$ inhibition by AnTTX and $96 \pm 0.5\%$ inhibition by both toxins consistent with the passage of much of the remaining current by $Na_v1.6$.

DOI: 10.7554/eLife.20054.003

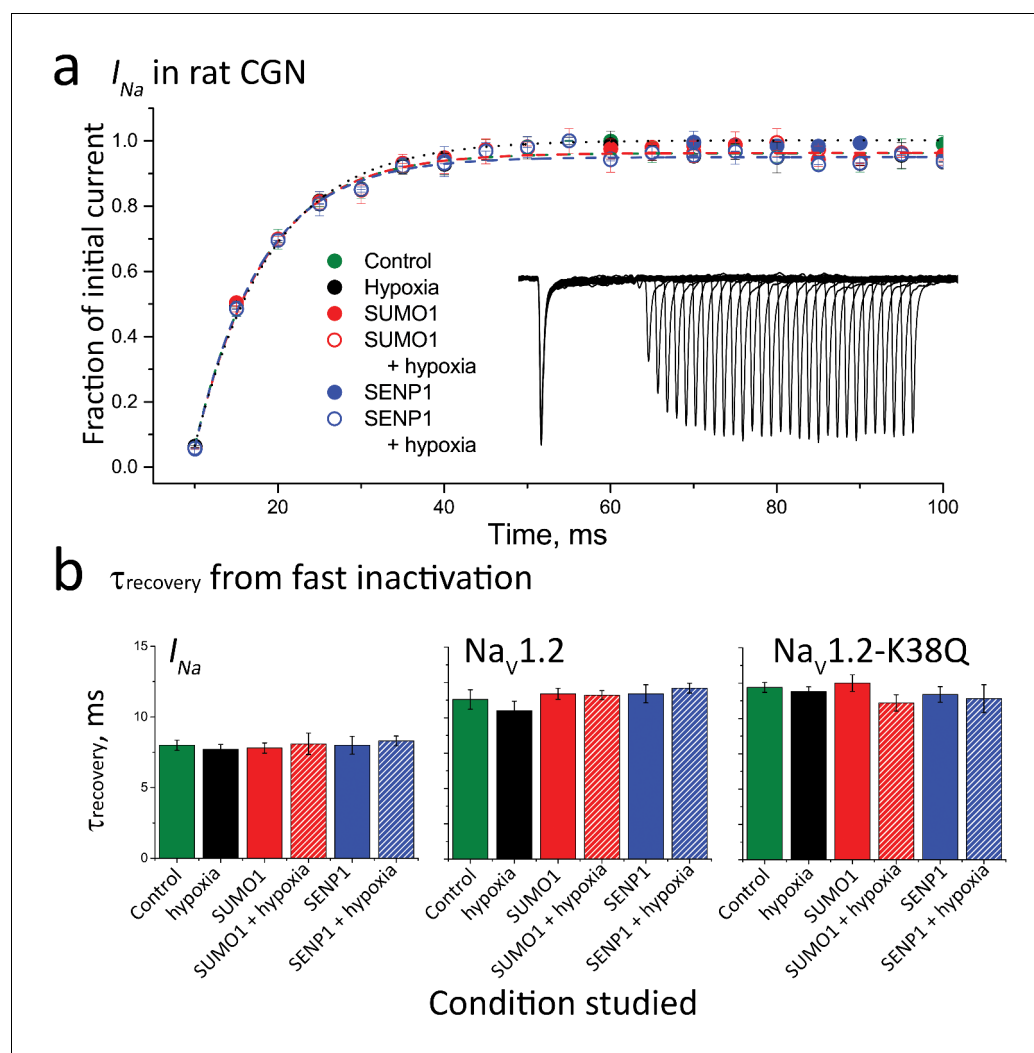


Figure 1—figure supplement 1. Recovery of I_{Na} and $Na_v1.2$ from fast inactivation is not altered by hypoxia, SUMO1 or SENP1. Neuronal I_{Na} or CHO cells expressing $Na_v1.2$ or $Na_v1.2$ -Lys38Gln ($Na_v1.2$ -K38Q) were studied in whole-cell mode. To assess recovery from fast inactivation cells were held at -100 mV, depolarized to -20 mV for 30 ms and then held at -100 mV for increasing amounts of time before a second 30 ms, -20 mV test pulse to measure the fraction of current recovered. Data are mean \pm S.E.M. for 6–10 cells per group. **(a)** The fraction of initial I_{Na} recovered in subsequent test pulses is plotted against the interpulse interval and fitted with a mono-exponential function to determine the time-constant (τ) of recovery. The mean time constant for control cells was 8 ± 0.36 (green) and did not differ when cells exposed to hypoxia (black) with or without 100 pm SUMO (red) or 250 pm SENP1 (blue) in the recording pipette. Inset; An example current, showing the recovery time course of I_{Na} recorded from a control neuron. **(b)** Histograms showing the mean τ of recovery, assessed as in **(a)**, for neuronal I_{Na} or $Na_v1.2$ or $Na_v1.2$ -K38Q expressed in CHO cells under the experimental conditions described. Neither the point mutation K38Q, nor treating cells with hypoxia, SUMO1 or SENP1 modulated recovery kinetics.

DOI: [10.7554/eLife.20054.004](https://doi.org/10.7554/eLife.20054.004)

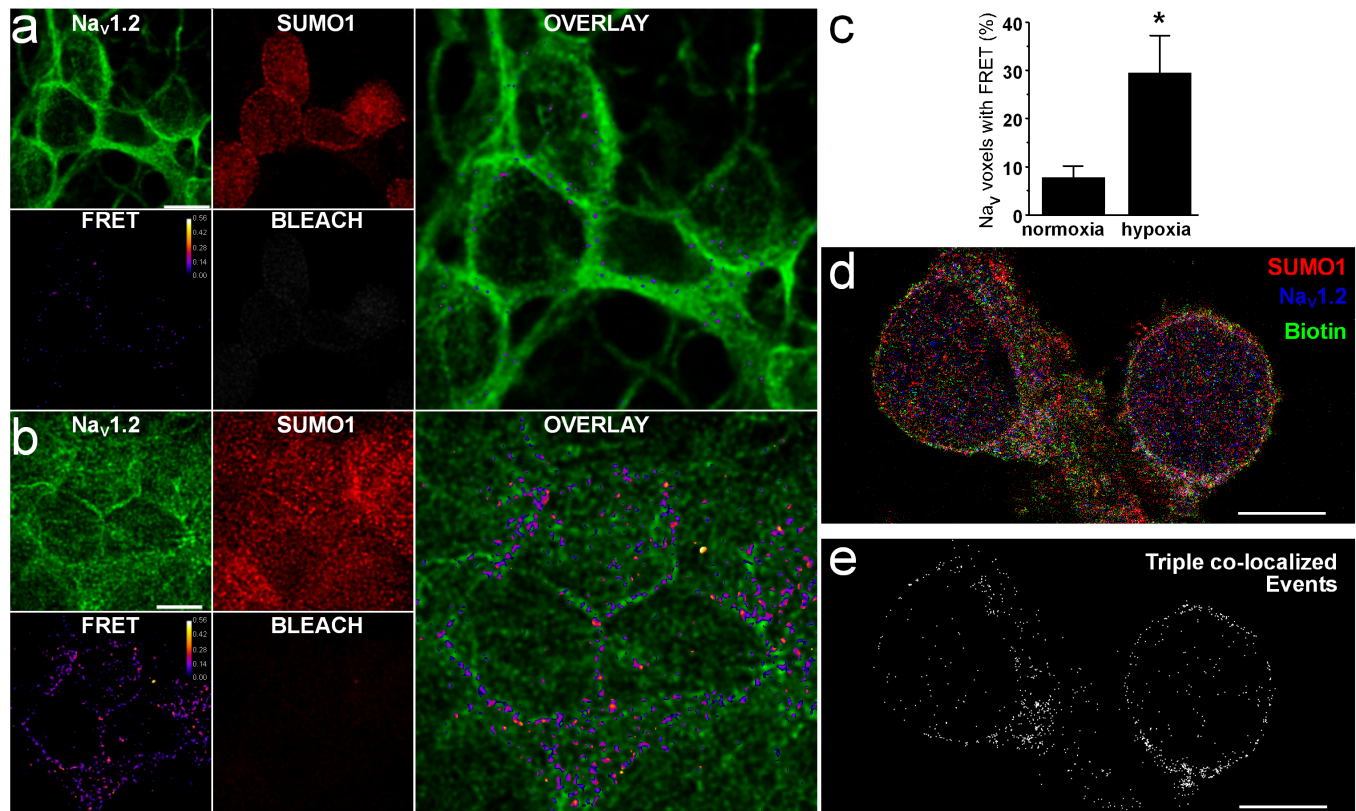


Figure 2. Na_v1.2 assembles with native SUMO1 at the surface in rat CGN. The association of native Na_v1.2 and SUMO1 in CGN was studied by amFRET and STORM per the Materials and methods. Data are mean ± S.E.M. The scale bar represents 5 μm. (a) Representative photomontage of amFRET of Na_v1.2 and SUMO1 in cells exposed to normoxia, using Alexa Fluor 488 and Alexa Fluor 594-labeled secondary antibodies to anti-Na_v1.2 and anti-SUMO1. The four smaller images show Na_v1.2 (donor, top left), SUMO1 (acceptor, top middle), the acceptor after photobleaching (BLEACH, bottom right), and FRET (bottom left, FRET efficiency indicated in pseudo-colored scale); the calculated FRET ratio in voxels after acceptor photobleaching was 0.15 ± 0.01 (n = 10 neurons on six coverslips). The large panel is an overlay of the donor and resultant FRET. (b) Representative photomontage of amFRET of Na_v1.2 and SUMO1 in cells exposed to hypoxia (1% O₂), using the identical approach and image layout as in panel a showing a calculated FRET ratio after acceptor photobleaching of 0.28 ± 0.05 (n = 8 neurons on five coverslips). (c) Histogram showing a four-fold increase in the voxels with Na_v1.2 demonstrating FRET from ambient conditions (7.8 ± 2.3%) with hypoxia (29.6 ± 7.6%, n = 8 on five coverslips); * indicates p < 0.001. (d) Composite scatterplot of fluorophore localizations obtained with STORM imaging. Maximum z-projections of scatterplots of fluorophore events from Alexa 568-labeled anti-SUMO1 antibodies (red), Alexa 647-labeled anti-Na_v1.2 antibodies, and Alexa 488-tagged streptavidin bound to extracellular membrane proteins are superimposed. Pixels are 20 nm square. (e) Mask of 20 nm square voxels in which fluorophore events from anti-SUMO1, anti-Na_v1.2 and streptavidin co-localize for exemplar neurons (n = 5).

DOI: [10.7554/eLife.20054.006](https://doi.org/10.7554/eLife.20054.006)

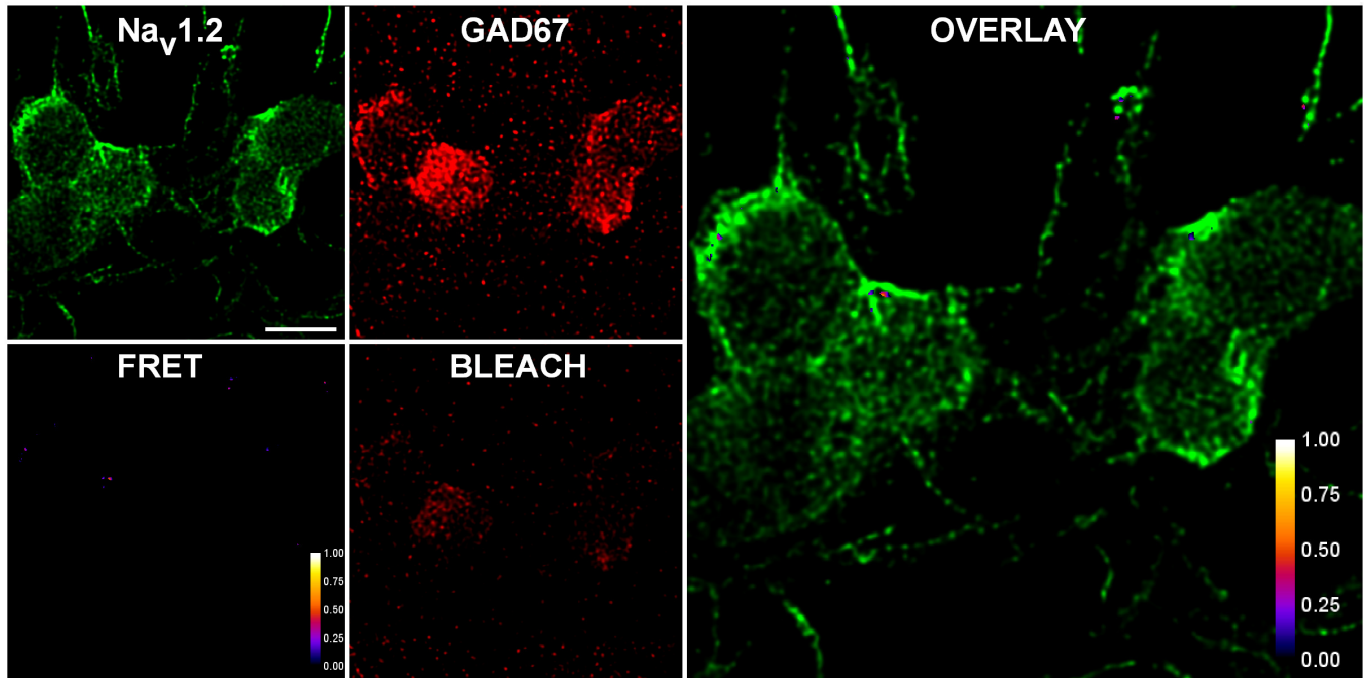


Figure 2—figure supplement 1. FRET was not observed between native Na_v1.2 and GAD67 in CGN. Native protein amFRET was performed between Na_v1.2 (green) and GAD67 (red) in ambient O₂ as described in **Figure 2** and the Materials and methods. Negligible FRET was observed. GAD67 was detected with a secondary antibody labeled with Alexa 594 (acceptor) and Na_v1.2 with Alexa 488 (donor).

DOI: [10.7554/eLife.20054.007](https://doi.org/10.7554/eLife.20054.007)

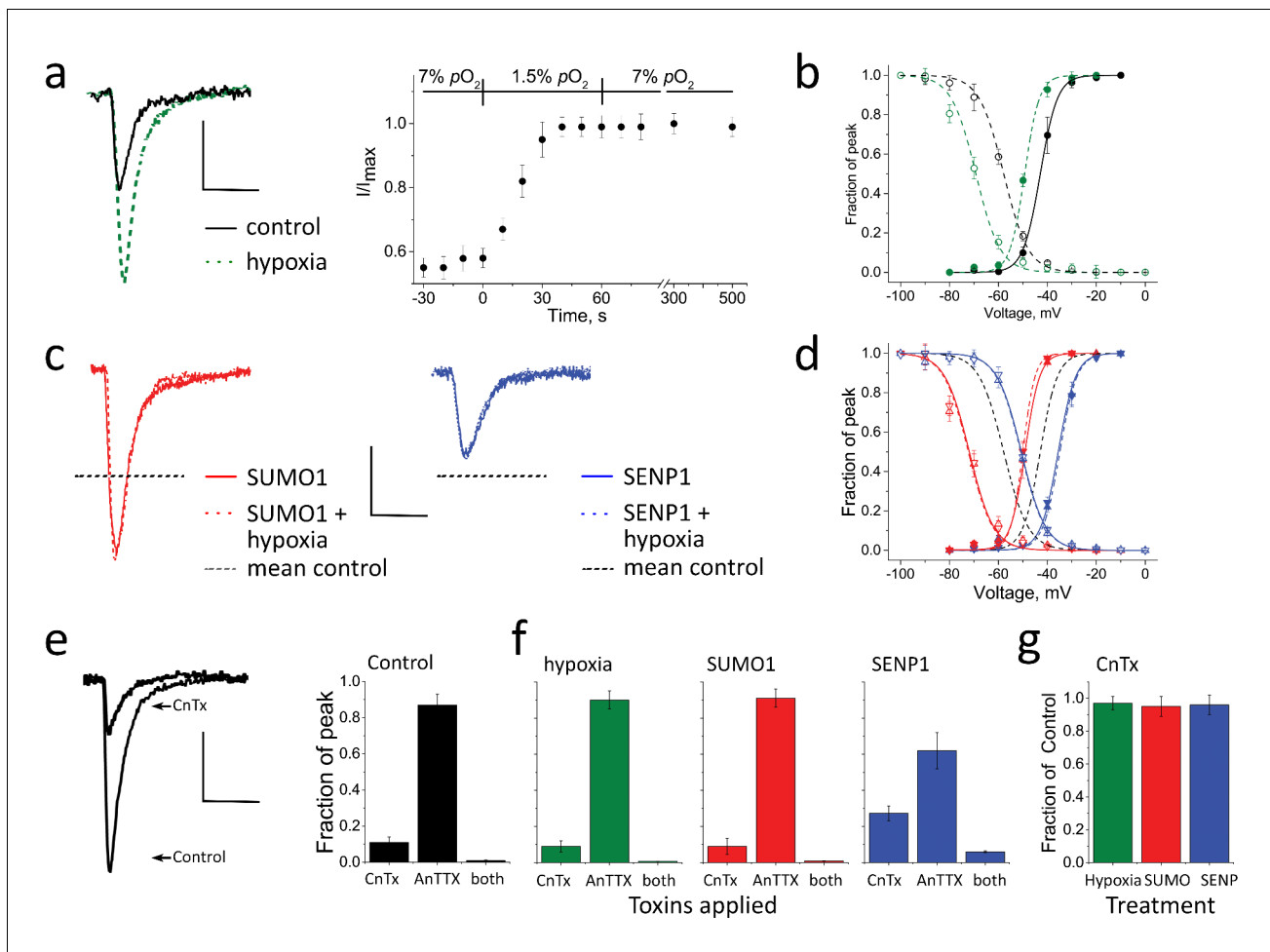


Figure 3. Acute hypoxia at 1.5% O_2 after culturing at 7% augments I_{Na} in rat CGN was studied following 5–7 days in culture at 7% O_2 by whole-cell patch clamp, as per **Figure 1**. Normalized activation (Act) and steady-state inactivation (SSI) relationships were obtained and fit as described in the Materials and methods. Measured values are noted in the text and listed in **Supplementary file 1b**. Cells were studied with a control solution (black), 100 pm SUMO1 (red), or 250 pm SENP1 (blue) in the recording pipette. Sensitivity to CnTx and AnTTX was assessed as per **Figure 1**. Data are mean \pm S.E.M. for six cells per group. Scale bars are 150 pA/pF and 5 ms. (a) Left, example traces showing I_{Na} at -20 mV increased when perfusate at 7% O_2 (black) was exchanged with a hypoxic solution at 1.5% O_2 (green dashes). Right, the time-course for changes in peak current in response to decreased O_2 from 7 to 1.5%, normalized to the maximal current for each cell studied. (b) Hypoxic solution (green dashes) left shifted the $V_{1/2}$ of I_{Na} from control (black) for both Act (solid) and SSI (open). (c) Left, SUMO1 in the pipette (red) increased I_{Na} and no further augmentation was observed by subsequent hypoxia (red dashes). Right, SENP1 in the pipette (blue) decreased I_{Na} and suppressed the response to hypoxia (blue dashes). Dotted black lines indicate the mean peak values obtained at 7% O_2 in a. (d) SUMO1 left shifted the $V_{1/2}$ of Act (red triangle) and SSI (open red triangle). The relationships were then insensitive to hypoxia (Act, red down triangle; SSI, open red down triangle). SENP1 right shifted the $V_{1/2}$ of Act (blue triangle) and SSI (open blue triangle) and currents were then insensitive to hypoxia. Dashed black lines indicate mean peak values with control solutions from b. (e) Left; I_{Na} studied at 7% O_2 then with toxins in the bath. Right; mean normalized peak current histograms showing $89 \pm 1.2\%$ inhibition by CnTx, $12 \pm 2\%$ inhibition by AnTTX and $99 \pm 0.8\%$ inhibition by both toxins (black bars). These ratios indicate that the relative contribution of $Na_v1.2$ and $Na_v1.6$ to I_{Na} is not altered when cells are cultured at 7% O_2 . (f) Mean normalized peak I_{Na} histograms. Left; $91 \pm 1\%$ inhibition by CnTx and $10 \pm 1\%$ inhibition by AnTTX with a drop to 1.5% O_2 for 60 s (green). Middle; $90 \pm 2\%$ inhibition by CnTx and $9 \pm 2\%$ inhibition by AnTTX with 100 pm SUMO1 in the pipette (red). When SENP1 was included in the recording pipette (blue), I_{Na} was inhibited by $73 \pm 3\%$ by CnTx, $38 \pm 8\%$ by AnTTX and $95 \pm 2\%$ by both toxins consistent with the passage of much of the remaining current by $Na_v1.6$. (g) Mean normalized peak current histograms show that the I_{Na} remaining after inhibition of $Na_v1.2$ by CnTx did not respond to acute hypoxia at 1.5% O_2 (green), SUMO1 (red), or SENP1 (blue).

DOI: 10.7554/eLife.20054.008

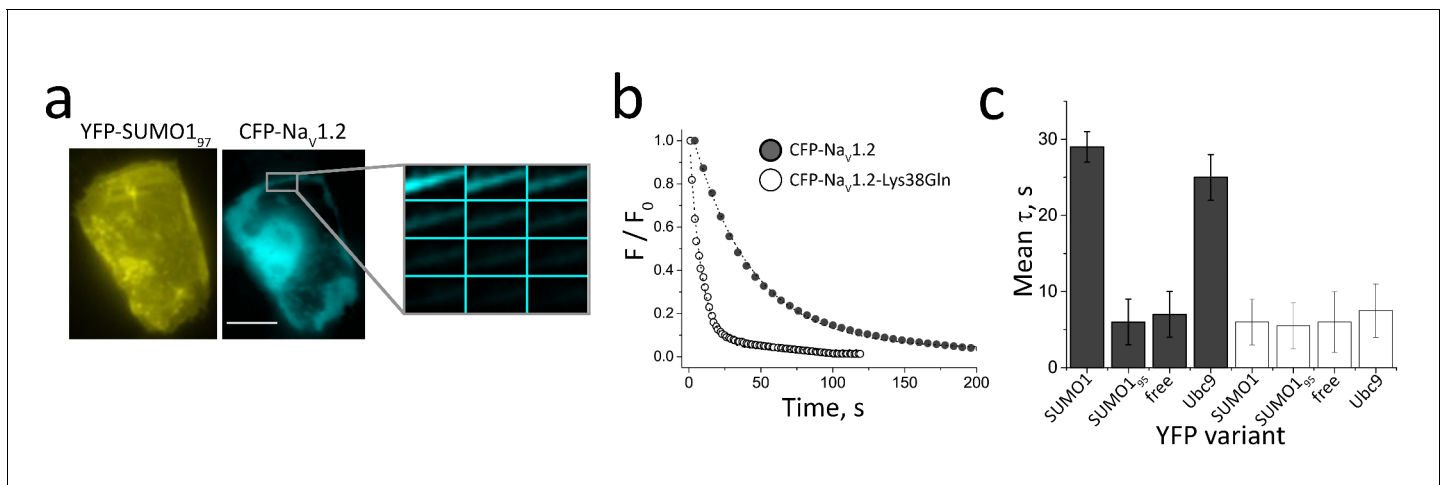


Figure 4. FRET between Nav1.2 and SUMO1 at the cell surface requires Lys38. Rat Nav1.2 was expressed in CHO cells with the β 1 subunit and studied in live cells per Materials and methods. FRET was assessed by measuring the time constant (τ) for CFP-photobleaching (donor) in the presence of YFP (acceptor) from 3 regions of 5–7 cells per group. Data are mean $\tau \pm$ S.E.M. (a) CFP-Nav1.2 subunits (blue) and YFP-SUMO1 (yellow) reach the cell surface. Scale bar is 10 μ m. (b) Exemplar photobleaching studies show the decay of fluorescence intensity for single cells expressing CFP-Nav1.2 (open) or CFP-Nav1.2-Lys38Gln (solid) with YFP-SUMO1 fit by an exponential to give τ . (c) FRET shows the assembly of CFP-Nav1.2 (grey bars) with YFP-SUMO1 and YFP-Ubc9 ($\tau = 29 \pm 2^*$ and $25 \pm 3^*$, respectively) but not with linkage-incompetent YFP-SUMO1₉₅ or free YFP ($\tau = 6 \pm 3$ and 7 ± 3 , respectively). In contrast, CFP-Nav1.2-Lys38Gln (white bars) did not show FRET with YFP-SUMO1, YFP-SUMO1₉₅, YFP-Ubc9 or free YFP ($\tau = 6 \pm 3$; 5.5 ± 3.5 ; 7.5 ± 3.5 ; and 6 ± 4 , respectively). Significant changes in τ compared to free YFP are indicated (*, $p < 0.001$).

DOI: [10.7554/eLife.20054.009](https://doi.org/10.7554/eLife.20054.009)

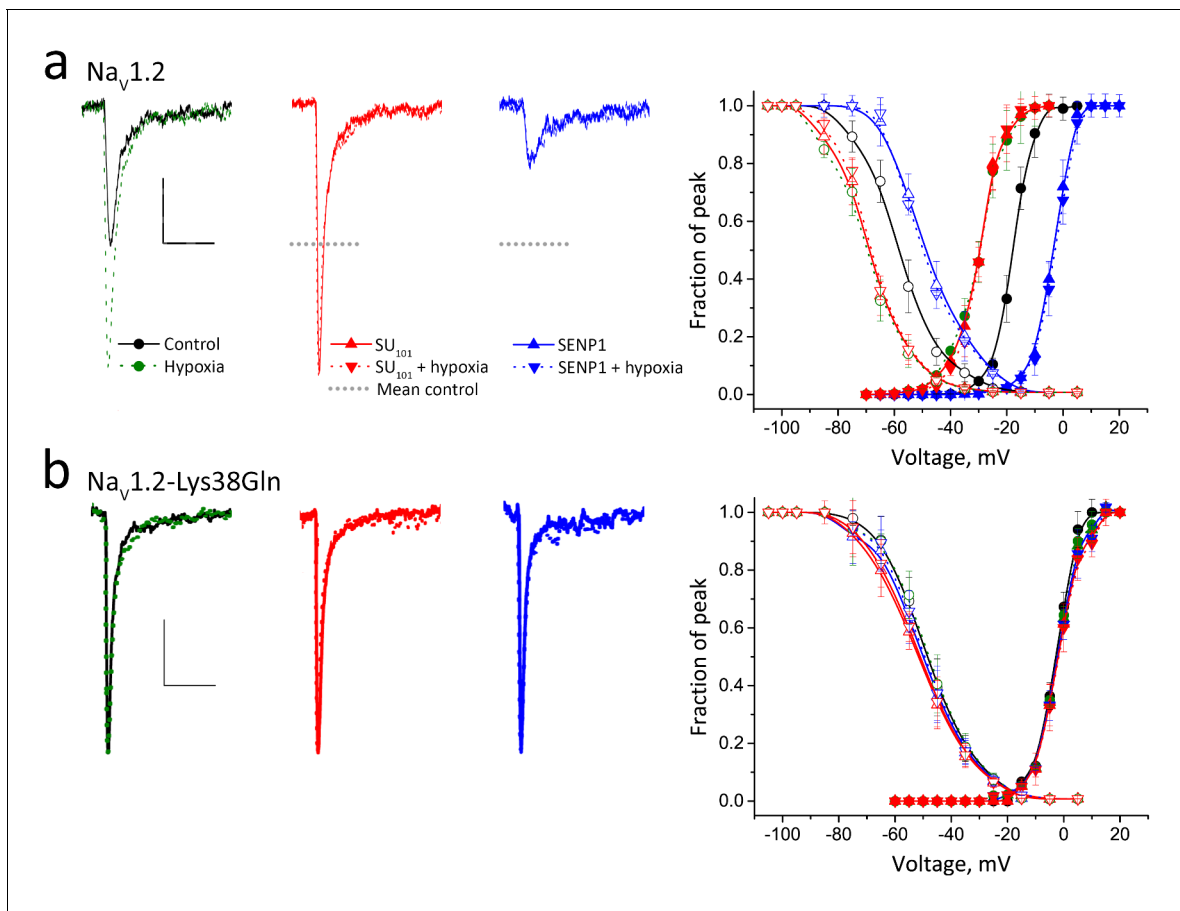


Figure 5. Acute hypoxia induces SUMOylation of Na_V1.2 on Lys38. Rat Na_V1.2 was expressed in CHO cells with the β 1 subunit and studied under normoxic and hypoxic conditions with control solution (black), 100 pm SUMO1 (red) or 250 pm SENP1 (blue) in the recording pipette, as indicated. Data are mean \pm S.E.M. for 10 to 15 cells per group. Measured values are noted in the text and listed in **Table 1**. Scale bars are 5 ms and 50 pA/pF in **a** and 10 pA/pF in **b**. **(a)** Left, example traces show hypoxia (green dashes) increased Na_V1.2 channel current from control conditions (black). SUMO1 in the pipette (red) increased the current to the same level and precluded further augmentation by hypoxia (red dashes). In contrast, SENP1 (blue) decreased the current by \sim 75% and suppressed sensitivity to hypoxia (blue dashes). Dotted black lines represent mean peak current under control conditions. Right, both Act (solid) and SSI (open) for Na_V1.2 were left shifted when cells with hypoxia (green) or SUMO1 in the pipette (red) and were right-shifted with SENP in the pipette (blue). Hypoxia caused no further change to Act or SSI with SUMO1 or SENP1 in the pipette (dashed lines). **(b)** Left, Na_V1.2-Lys38Gln channels passed smaller currents (black) that were not increased by hypoxia (green) or by SUMO1 in the pipette (red) or decreased by SENP1 (blue) in the pipette. Right, the normalized Act and SSI relationships for Na_V1.2-Lys38Gln channels (black) are right-shifted compared to wild type Na_V1.2 channels and do not change when cells are exposed to hypoxia (green) or are studied with SUMO1 (red) or SENP (blue) in the pipette.

DOI: 10.7554/eLife.20054.010

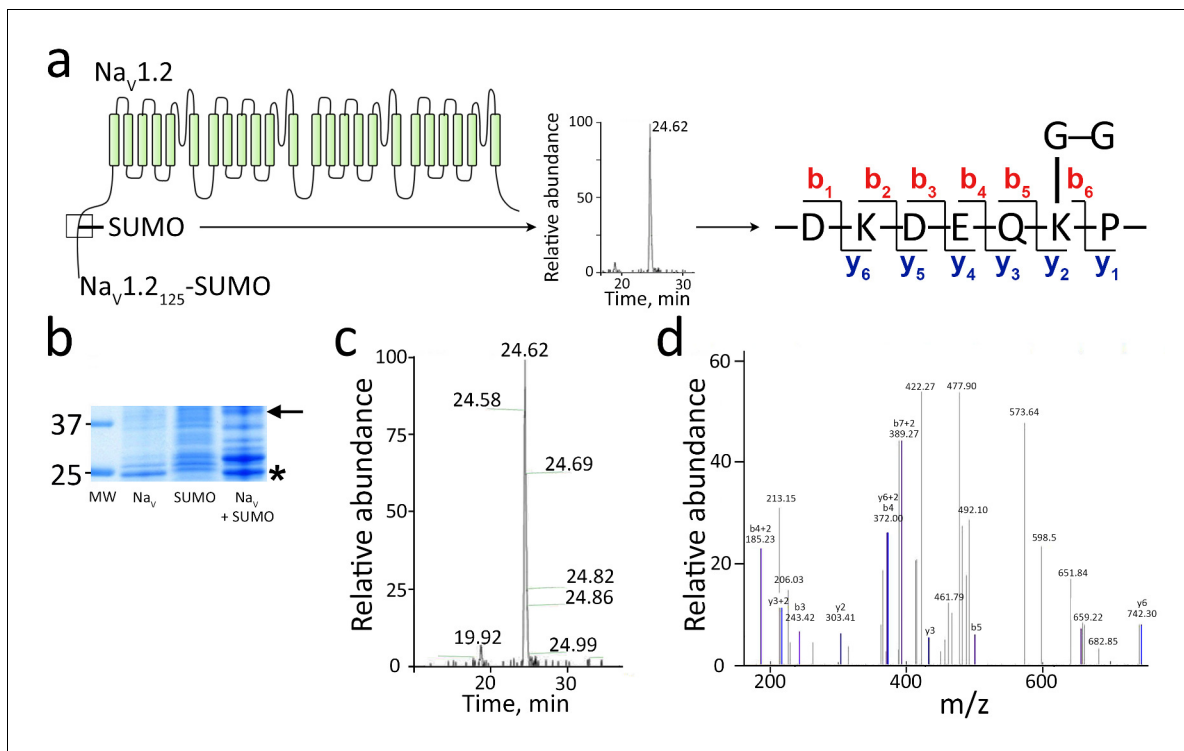


Figure 6. Mass spectrometry shows SUMO1 conjugated to Nav_v1.2-Lys38. For MS analysis, rat Nav_v1.2₁₋₁₂₅ and SUMO1_{97T95K} were expressed with mouse SUMOylation enzymes in *E. coli*, purified, subjected to trypsin cleavage, and analyzed by MS as described in the Materials and methods. (a) Left, schematic showing the product Nav_v1.2₁₋₁₂₅-SUMO (box) and the tryptic fragment of Nav_v1.2 carrying the Gly-Gly remnant of SUMO1_{97T95K}. Right, The sequence of the three-ended fragment with Lys38 and the Gly-Gly remnant. (b) A Coomassie blue-stained SDS-PAGE gel of the purified products. Unmodified Nav_v1.2₁₋₁₂₅ (Na_v) migrates at ~25 kDa (star). Expression of SUMO1_{97T95K} (SUMO) and the SUMO enzymes yields SUMO on the overexpressed target as well as native proteins (Plant et al., 2011; Uchimura et al., 2004). The Nav_v1.2₁₋₁₂₅-SUMO conjugate migrates at ~40 kDa (arrow). Molecular weight markers are shown (MW). (c) Fourier transform mass spectrum after trypsin digestion of Nav_v1.2₁₋₁₂₅-SUMO expressed as relative abundance against time of capture. The predicted fragment of 422.27 Da was captured as a single peak at 24.62 min. (d) Tandem MS sequence analysis of the fragment with Lys38 and the Gly-Gly remnant indicating b and y ion species as annotated in a.

DOI: 10.7554/eLife.20054.011

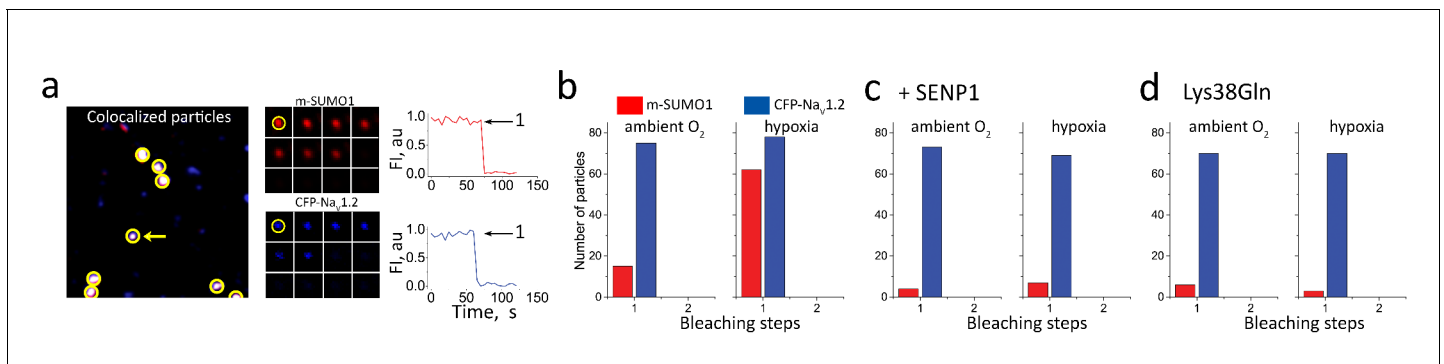


Figure 7. Hypoxia recruits one SUMO1 monomer to each cell surface Nav1.2 channel. Single CFP-Nav1.2 or CFP-Nav1.2-Lys38Gln (K38Q, blue) channels and SUMO1 tagged with mCherry (m-SUMO1, red) were studied in CHO cells by TIRFM as described in the Materials and methods. Data represent 5–8 cells in each case and biophysical parameters and single particles statistical analyses are summarized in **Supplementary file 1a** and **Table 2**, respectively. (a) Left, single co-localized particles with both mCherry and CFP fluorescence were observed at the surface of cells expressing Nav1.2 and SUMO1. Simultaneous continuous photobleaching time courses revealed complexes to have one subunit of each type. (b) Histogram of photobleaching steps showing that hypoxia increased single mCherry-SUMO1 (red) subunits at the cell surface co-localized with Nav1.2 channels (blue), without a change in subunit stoichiometry (**Table 2**). (c) Histogram of photobleaching steps showing that SENP suppresses hypoxia-induced increase in single mCherry-SUMO1 (red) subunits at the cell surface co-localized with Nav1.2 (blue). (d) Histogram of photobleaching steps showing that hypoxia does not increase in single mCherry-SUMO1 (red) subunits at the cell surface co-localized with Nav1.2-Lys38Gln channels (blue).

DOI: [10.7554/eLife.20054.012](https://doi.org/10.7554/eLife.20054.012)

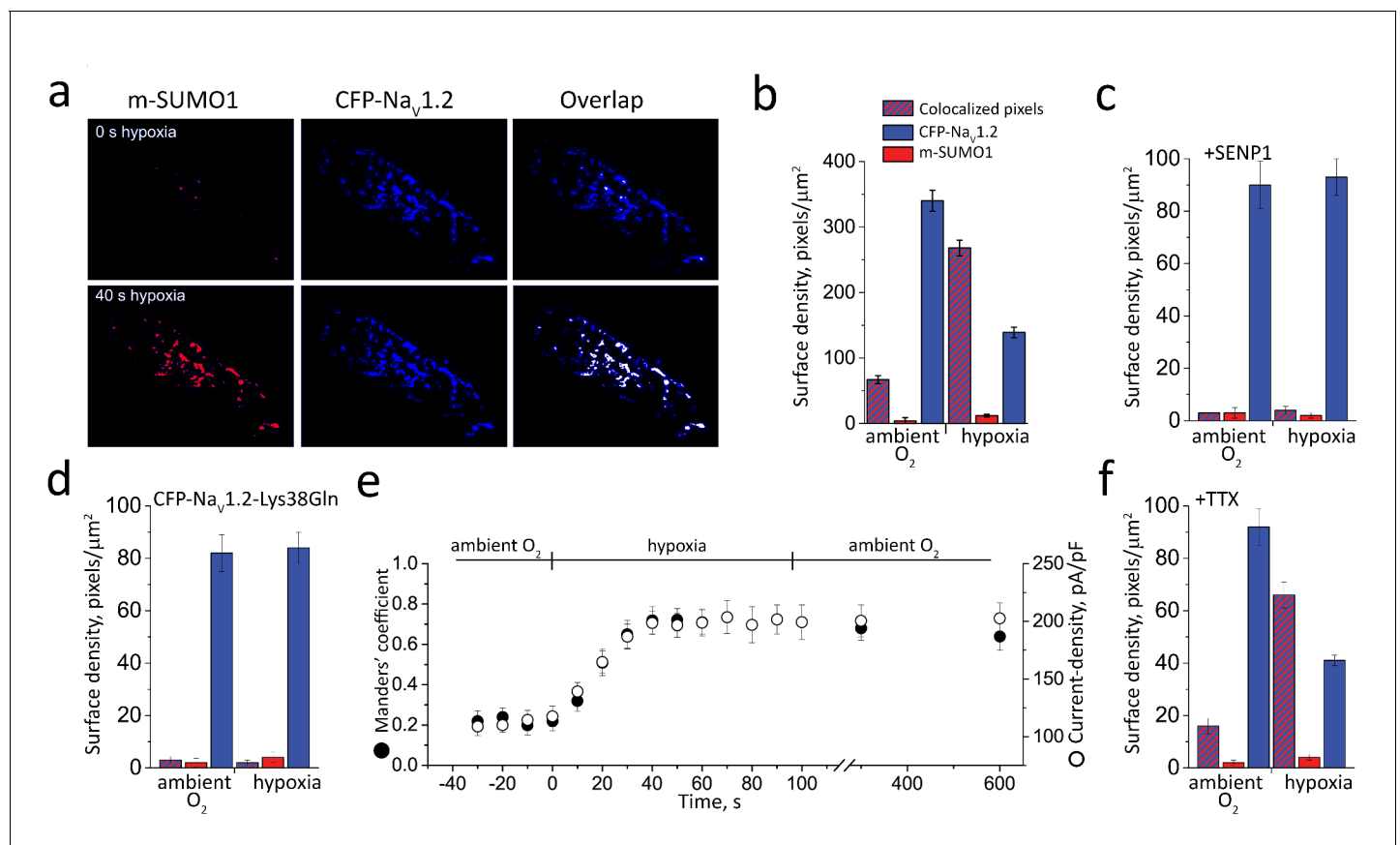


Figure 8. Hypoxic SUMOylation of Nav1.2 and current density proceed concurrently. CFP-Nav_v1.2 or CFP-Nav_v1.2-Lys38Gln (K38Q, blue) channels and SUMO1 tagged with mCherry (m-SUMO1, red) were studied in CHO cells by TIRFM and pixel-by-pixel analysis performed as described in the Materials and methods. Briefly, images were captured at 5 s intervals and data for each fluorophore saved as separate stacks; the background was subtracted and processed for misalignment in an identical manner. Manders' coefficients were assessed post-hoc for 3–5 regions per cell. Co-localization was defined as the presence of both fluorophores at more than 30% of the maximum fluorescence level recorded in that stack (and their overlap is represented in the images as white pixels). The time-course of hypoxic modulation of Nav_v1.2 current in moving from O₂ of 21% to 5% was studied with steps from –100 mV to –20 mV every 10 s and normalized to cell capacitance (pA/pF). Data represent 5–8 cells and biophysical parameters and single particles statistical analyses are summarized in **Supplementary file 1a** and **Table 2**, respectively. (a) Hypoxia rapidly recruits SUMO1 to the cell surface at sites with Nav_v1.2 channels. The images show that the surface density of m-SUMO1 (top, left) is low compared to CFP-Nav_v1.2 (top, middle) with little co-localization (top, right) in ambient O₂. After 40 s of hypoxia, rapid recruitment of SUMO1 (bottom, left) to the surface is observed to be at sites with Nav_v1.2 channels (bottom, left). Surface levels of Nav_v1.2 were not observed to change when cells were exposed to hypoxia (bottom, middle). (b) Histogram of surface density summarizing seven cells studied as described in **a** and **Table 2**. The density of pixels per μm² with SUMO1 alone (red) was 4 ± 5, with Nav_v1.2 alone (blue) was 340 ± 16, and with both subunits was 67 ± 6 (red/blue hatch). Hypoxia increased co-localization to 268 ± 12 pixels per μm² and decreased the density of free Nav_v1.2 channels (139 ± 8) without altering the density of free SUMO1 (12 ± 2). (c) The hypoxia-induced increase in the surface density of single fluorescent particles with both SUMO1 and Nav_v1.2 was not observed in cells with 100 nm SENP1 in the pipette. (d) Hypoxia-induced increase in the surface density of SUMO1 was not observed in cells expressing CFP-tagged Nav_v1.2-Lys38Gln (K38Q). (e) The time-course for hypoxia-induced increase co-localization of Nav_v1.2 and SUMO1 (Manders' coefficient, solid circle) and current-density (pA/pF, open circle) were coincident. The mean Manders' coefficient of 0.22 ± 0.08 measured in ambient O₂ increased to 0.72 ± 0.12 in less than 40 s of acute hypoxia. The current density increased from –120 ± 8 to 198 ± 10 pA/pF. Increases in the Manders' coefficient and current density were unchanged 10 min after cells were restored to ambient O₂. (f) Hypoxia-induced increase in the surface density of colocated SUMO1 and Nav_v1.2 was also observed when cells were treated with 5 μM tetrodotoxin (TTX), a level that blocked over 95% of the Na⁺ current.

DOI: [10.7554/eLife.20054.014](https://doi.org/10.7554/eLife.20054.014)